Astron. Astrophys. 321, 389–396 (1997)

ASTRONOMY
AND
ASTROPHYSICS

A search for molecular gas in high redshift radio galaxies

R. van Ojik[1], H.J.A. Röttgering[1,2,3], P.P. van der Werf[1], G.K. Miley[1], C.L. Carilli[1,4], A. Visser[1], K.G. Isaak[2], M. Lacy[5], T. Jenness[2], J. Sleath[2], and J. Wink[6]

[1] Leiden Observatory, P.O. Box 9513, 2300 RA Leiden, The Netherlands
[2] Mullard Radio Astronomy Observatory, Cavendish Laboratory, Cambridge CB3 0HE, UK
[3] Institute of Astronomy, Madingley Road, Cambridge CB3 0HA, UK
[4] NRAO, P.O. Box 0, Socorro, NM 87801, USA
[5] Astrophysics, Department of Physics, Keble Road, Oxford, OX1 3RH, UK
[6] Institut de Radioastronomie Millimétrique, 300 Rue de la Piscine, F-38406 St. Martin d'Hères Cedex, France

Received 18 December 1995 / Accepted 27 September 1996

Abstract. We present results of an extensive search for molecular gas in 14 high redshift ($z > 2$) radio galaxies. Radio galaxies with redshifts between 2.0 and 4.3 were observed during several sessions on two different single-dish telescopes (IRAM and JCMT) and two interferometric arrays (VLA and OVRO). No significant CO emission to a 2σ limit of a few times 10^{10} K km s^{-1} pc^2 was detected in any of these objects. The limits on the CO emission achieved indicate that, assuming a CO-H_2 conversion factor similar to the Galactic value, the mass of enriched molecular gas in these galaxies is less than 10^{11} M$_\odot$. This suggests that distant radio galaxies may not be forming stars at the extremely high rates that have earlier been proposed, although they may still be forming stars at rates comparable to those of local starburst galaxies.

Key words: galaxies: active – galaxies: ISM – radio lines: galaxies – radio continuum: galaxies

1. Introduction

One of the key questions in the evolution of galaxies concerns the epoch of maximum star formation. Since in the Milky Way star formation takes place in molecular clouds, the presence of large amounts of molecular gas in distant galaxies would be an indication that they are undergoing prodigious star formation. For this reason it is important to find and study molecular gas in the most distant galaxies.

The first high redshift galaxy to be detected in molecular emission lines was IRAS F10214+4724 at $z = 2.286$ (Rowan-Robinson et al. 1991). Several CO lines were detected (Brown & Vanden Bout 1991, Solomon et al. 1992a) which would indicate a molecular gas mass of $\sim 10^{11}$ M$_\odot$[1], dominating the dynamical mass. However, recently it was discovered that IRAS F10214+4724 is gravitationally lensed (Broadhurst & Lehár 1995, Graham & Liu 1995). Given the estimated lensing factor between 3 and 20, its true molecular gas mass may be only $\sim 10^{10}$ M$_\odot$. Since the discovery of CO emission from IRAS F10214+4724, confirmed molecular line emission has been detected in one other high redshift object, the also gravitationally lensed "Cloverleaf" quasar H 1413+117 at $z = 2.5$ (Barvainis et al. 1994). In spite of the uncertain lensing factor (estimated ~ 7) this quasar must also contain a large amount of molecular gas. Noteworthy is that both the Cloverleaf quasar and IRAS F10214+4724 have an AGN-type spectrum (see Elston et al. 1994), i.e., a spectrum with high ionization lines produced by a hard ultraviolet continuum. In spite of this ionizing continuum there is a large mass in molecular gas apparently shielded from the UV radiation so that the molecules can survive.

In addition, there have been reports on possible CO emission from damped Lyα absorption systems (Brown & Vanden Bout 1993, Frayer et al. 1994), but more sensitive observerations could not confirm these (Braine et al. 1996, Wiklind and Combes 1994).

The discovery of the strong CO emission from IRAS F10214+4724 indicated that it might be possible to observe molecular gas out to the highest currently known redshifts and suggested that many high redshift objects might contain large amounts of molecular gas. High redshift radio galaxies (HZRGs) usually have very bright Lyα emission, with integrated fluxes of $\sim 10^{-15}$ erg s^{-1} cm^{-2} (luminosities 10^{44} erg s^{-1}), and can extend over more than $10''$ (~ 100 kpc), indicating the presence of a large reservoir of gas in and around

Send offprint requests to: H.J.A. Röttgering (Leiden address)

[1] Throughout this paper we assume a Hubble constant $H_0 = 100$ km s^{-1} Mpc^{-1} and a deceleration parameter $q_0 = 0.5$; values quoted from other papers are, where necessary, tacitly converted to this cosmology.

these galaxies. The importance of HZRGs for the formation and evolution of galaxies in general is shown by the fact that radio galaxies were almost a thousand times more common at $z \sim 2$ than at the current epoch. The bright emission lines in the optical spectra of HZRGs are a factor of $5-10$ narrower than those of quasars, facilitating an accurate determination of their redshifts, which is a prerequisite for deep mm-wave spectroscopy due to the limited spectral bandwidth of current instrumentation.

It has been proposed that HZRGs are protogalaxies undergoing their first major burst of star formation (see Eales and Rawlings 1993, and references therein). At low redshifts, radio galaxies have molecular gas masses of the order of $10^{10}\,M_\odot$ (Mazzarella et al. 1993). Such masses are comparable to those of known luminous infrared starburst galaxies like Arp 220 (Solomon et al. 1990). High redshift radio galaxies have been suspected of having vigorous starbursts associated with the propagation of the radio jet (Rees 1989, Begelman & Cioffi 1989) as one of the explanations of the alignment of the optical, infrared and radio axes found in HZRGs (Chambers et al. 1987, McCarthy et al. 1987), although alternatives have been proposed as well (cf., Sect. 4.2). The starburst model proposed by Chambers and Charlot (1990) requires the formation of $10^{11}\,M_\odot$ of stars over 10^7 yr. Such starbursts should be accompanied by the production of large amounts of heavy elements, giving rise to the formation of copious amounts of dust and molecules. Evidence for the presence of dust comes from polarization measurements of HZRGs (e.g., Tadhunter et al. 1992; Cimatti et al. 1993) and detections of continuum emission from dust at submillimetre wavelengths (Dunlop et al. 1994, Ivison 1995). The detection of large amounts of molecular gas in such objects would be strong evidence in favour of the massive starburst hypotheses.

In an extensive survey of ultrasteep spectrum radio sources we have found 29 radio galaxies at $z > 2$ (van Ojik et al. 1994, van Ojik et al. 1996a, Röttgering et al. 1995a, Röttgering et al. 1997), a significant fraction of the total number of radio galaxies known at such high redshifts. The large luminosities of the observed emission lines indicate that there is a powerful source of ionizing radiation in such objects, albeit hidden from the observers. Any molecular gas would have to be shielded from this ionizing radiation (as in IRAS F10214+4724 and the Cloverleaf quasar) to prevent the molecules from dissociating. The anisotropic ionizing radiation is most likely oriented in a cone along the radio axis (Antonucci 1993). Thus most molecular gas might be situated outside this cone of ionizing radiation and is likely undisturbed by the radio jet, which may be responsible for the large velocity dispersions of the extended optical emission line gas (Van Ojik et al. 1997). Thus, we may expect any CO emission lines to be much narrower than the optical emission lines (which have typically $1000\,\mathrm{km\,s^{-1}}$ FWHM) and similar in width to the CO line widths observed both in IRAS F10214+4724 and the Cloverleaf quasar ($\sim 300\,\mathrm{km\,s^{-1}}$ FWHM). We here report on our search for molecular gas in 14 HZRGs.

Table 1. Single-dish observing sessions

Session	Date	Telescope	Time [hours]	Comments
1	Nov 1993	JCMT	56	
2	Nov 1993	IRAM	20	variable conditions
3	Jan 1994	IRAM	28	
4	Apr 1994	JCMT	24	
5	Jun 1994	JCMT	40	variable conditions
6	Aug 1994	IRAM	103	variable conditions
7	Dec 1994	JCMT	88	
8	Apr 1995	IRAM	55	variable conditions

2. Observations and reduction

2.1. Transitions surveyed

Our targets have redshifts ranging from 2.0 to 4.3. Taking into account the instrumentation available, this allowed us to survey CO transitions from $J = 3\rightarrow2$ (345.8 GHz rest frequency) for the objects with $z \sim 2$ observed at IRAM or the Owens Valley Radio Observatory millimeter interferometer (OVRO) in the 3 mm window, to $J = 9\rightarrow8$ (1036.9 GHz rest frequency) for the objects with the highest redshifts observing at the JCMT in the 1.3 mm window. With the VLA the CO $J = 1\rightarrow0$ transition can be observed at 25 GHz for the sources with the highest redshifts.

Strategies for detecting CO at high z have been discussed by Van der Werf and Israel (1996), who show that if conditions in these objects are similar to those in local starburst galaxies, the J=3→2 to J=6→5 lines are the transitions of choice in detection experiments. Significantly, the line ratios found in IRAS F10214+4724 and the Cloverleaf quasar are indeed similar to those in local starburst galaxies (Solomon et al. 1992a, Barvainis et al. 1994).

With the exception of B2 0902+34 (Lilly 1988) and 8C 1435+635 (Lacy et al. 1994), which were included because of their thermal dust emission (Chini & Krügel 1994, Ivison 1995), the sources observed were selected from the Leiden sample of HZRGs. One target, 0211−122, has an optical spectrum similar to that of IRAS F10214+4724, with strongly absorbed Lyα indicating the presence of dust (van Ojik et al.1994). Four other targets were selected because they showed evidence for associated H I absorption (Van Ojik et al. 1997; Röttgering et al. 1995a) and the remaining targets were selected because of their large Lyα halos and high redshifts. Thus, the 14 objects we observed are representative of our general sample of HZRGs.

2.2. Single-dish observations

We observed the sources in 8 different observing sessions, summarized in Tables 1 and 2.

Four sessions were carried out with the James Clerk Maxwell Telescope (JCMT) on Mauna Kea, Hawaii. We used the SIS receiver A2 tuned so that the redshifted frequency of the most suitable CO transition for each object, at 220 to 250 GHz,

Table 2. Log of the single-dish CO observations, with the r.m.s. noise σ in the spectrum given at a velocity resolution of 100 km s^{-1}.

Source	z	Session	Line	$t_{\rm int}$ [hours]	σ $T_{\rm mb}$ [mK]
0211−122	2.336	1	CO(7–6)	25.0	2.0
		2	CO(3–2)	4.0	1.2
		2	CO(4–3)	3.6	1.3
		6	CO(3–2)	1.5	2.0
		6	CO(4–3)	1.5	2.0
		6	CO(7–6)	1.5	2.4
		7	CO(7–6)	14.3	1.2
0214+183	2.131	7	CO(6–5)	1.7	2.3
0355−037	2.153	7	CO(6–5)	3.0	2.3
0448+091	2.040	7	CO(6–5)	2.0	1.3
4C 41.17	3.800	2	CO(4–3)	7.4	0.5
		2	CO(6–5)	7.6	0.4
0748+134	2.410	6	CO(3–2)	4.8	0.5
		6	CO(4–3)	4.8	3.0
		6	CO(7–6)	4.8	2.1
		7	CO(7–6)	2.3	1.9
0828+193	2.572	3	CO(3–2)	1.5	1.4
		3	CO(5–4)	1.5	1.7
		6	CO(3–2)	1.9	1.5
		6	CO(5–4)	1.9	3.8
		7	CO(7–6)	2.3	1.3
B2 0902+34	3.395	2	CO(4–3)	3.6	0.6
		2	CO(5–4)	5.6	0.8
0943−242	2.918	4	CO(8–7)	14.2	1.6
1243+036	3.570	3	CO(4–3)	3.9	1.2
		3	CO(6–5)	3.9	1.1
		4	CO(9–8)	14.2	1.0
		5	CO(9–8)	26.8	2.8
		6	CO(4–3)	6.1	2.8
		6	CO(6–5)	6.1	6.4
		8	CO(4–3)	35.1	0.6
1435+635	4.257	6	CO(4–3)	7.1	0.4
		6	CO(5–4)	7.1	2.2
1707+105	2.345	3	CO(3–2)	0.9	0.9
		3	CO(4–3)	0.9	1.3
2202+128	2.704	7	CO(8–7)	2.0	1.6
2251−089	2.000	7	CO(6–5)	1.9	2.2

was in the upper sideband. The telescope half-power beam width (HPBW) at these frequencies is about 20″. As backend we used the 2048 channel Dutch Autocorrelation Spectrometer with a bandwidth of 750 MHz. The single sideband (SSB) system temperatures in good atmospheric conditions were 300 to 450 K. We chopped the subreflector at 2 Hz with a throw of $\sim 60''$ and applied beam-switching.

Four sessions were carried out with the IRAM 30 m telescope at Pico Veleta, Spain. Usually, two or three receivers were used simultaneously, so that up to three CO transitions could be observed with high net observing efficiency. Two 512 channel, 512 MHz wide filter banks were used as backend for the 3 mm and 2 mm receivers and an autocorrelator backend for the 1.3 mm receiver. The HPBW was 25″ at 3 mm, 17″ at 2 mm and 11″ at 1.3 mm. The subreflector was chopped at 0.5 Hz with a throw of 120″. System temperatures at IRAM under reasonable weather conditions were $200-400$ K at 100 GHz, $300-500$ K at 150 GHz and ~ 1000 K at 230 GHz (SSB).

Table 3. Log of interferometric CO observations, with the r.m.s. noise σ in the spectrum given at a velocity resolution of 100 km s^{-1}.

Source	z	Telescope	Line	$t_{\rm int}$ [hrs]	σ [mJy beam^{-1}]
1243+036	3.5856	OVRO	4–3	32	1.6
1243+036	3.5856	VLA	1–0	18	0.6
1435+635	4.2576	VLA	1–0	10	0.3

The instantaneous velocity coverage of a spectrum ranged from 500 km s^{-1} (JCMT at 230 GHz) to 1200 km s^{-1} (IRAM 30 m at 100 GHz). The CO lines from our HZRGs are expected to be faint and broad, probably of the order of 300 km s^{-1}, covering a large portion of an instantaneous spectrum. Thus, broad low level ripples in the baseline of the spectra are a serious limitation in detecting these lines. In order to minimize baseline problems, integrations were carried out at several different local oscillator (LO) settings. By extending the covered baseline, residual baseline undulations should be better distinguishable and not be mistaken for true CO emission. Usually the LO settings were at 0, +150 and −150 km s^{-1} with respect to the calculated redshifted CO sky frequency, but occasionally we extended the baseline to 600 km s^{-1} from the nominal sky frequency. In this way we achieved a total velocity range of $\sim 1200-2000$ km s^{-1}.

Reduction of the spectra from IRAM was done with the CLASS (Continuum and Line Analysis Single-dish Software) reduction package, while the JCMT spectra were processed with the SPECX spectral line reduction package. The observations of each observing shift and each velocity setting were examined separately before summing them into a final spectrum. Scans with instrumental problems (e.g., curved baselines) or taken in poor conditions (atmospheric opacity $\tau > 0.2$) were discarded. The final spectra were smoothed with a 100 km s^{-1} FWHM Gaussian (i.e., a factor of $2-3$ smaller than the expected width of any CO emission line), and resampled. The antenna temperatures were converted to Rayleigh-Jeans main beam brightness temperature outside the atmosphere ($T_{\rm mb}$ [K]). The corresponding flux density scale for a point source with the JCMT is 18.9 Jy K^{-1} and with the IRAM telescope 4.7 Jy K^{-1} at 3 and 2 mm and 4.8 Jy K^{-1} at 1.3 mm.

2.3. Interferometric observations

Several systematic effects which limit deep spectroscopy using single-dish radio telescopes are reduced or absent for interferometric measurements, since interferometers only record correlated signals and are thus not sensitive to artefacts arising in separate elements. Two targets were therefore observed with interferometric arrays to verify the reality of apparent emission features found during single-dish measurements.

The VLA was employed to search for CO emission from two of the highest redshift objects, 1243+036 (z = 3.6) and 1435+635 (z = 4.3). The VLA has the advantage of a large collecting area and sensitive receivers, but the disadvantage of a limited bandwidth (50 MHz maximum, or 650 km s^{-1} at z = 4). Moreover, limitations in the IF system at the VLA constrain observations using a 50 MHz bandwidth to a discrete set of central frequencies, in sequential steps of 20 MHz and 30 MHz. For our observations we used a series of overlapping 50 MHz bands centered around the nominal systemic redshift, with 8 spectral channels per band and two circular polarizations, synthesizing a total bandwidth of 130 MHz for 1435+635 and of 80 MHz for 1243+036. The observational cycle included a sequence of short (5 minute) scans at each frequency setting, with scans on a nearby phase calibrator before and after each source scan.

The source 1435+635 was observed in the D-array (1 km maximum baseline) in May 1995. The phase calibrator was 1435+638, and 3C 286 was used for gain and bandpass calibration. Four frequency settings were used implying a total redshift range searched for emission of 4.2420 to 4.2732 (observing frequencies around 21.9 GHz). The source 1243+036 was observed during reconfiguration from C array (3 km maximum baseline) to D array in October 1995. Only the D-array spacings were employed in the final analysis in order to limit problems with phase coherence. The source 3C 273, which is located conveniently close to 1243+036 at an angular distance of only 5°, was used for phase and bandpass calibration, and 3C 286 was used for gain calibration. Three frequency settings were employed, implying a redshift range searched for emission of 3.5784 to 3.5932. The observing frequencies were around 25.1 GHz for this source. This frequency is at the edge of the VLA K-band, leading to LO phase lock problems on some antennas, and to a generally higher noise level (by a factor 2.5 or so relative to the K-band center). In the end, only 17 antennas were used in the analysis. The beam (FWHM) of the VLA (in hybrid configuration BnC for 1243+036 and DnC for 1435+635) was about 2.5″ at 22 GHz. This beam size is similar to the extent of optical continuum emission.

Standard phase, amplitude, and bandpass calibration was employed using the Astronomical Image Processing System (AIPS) at the U.S. National Radio Astronomy Observatory, Socorro. Spectral channel images were constructed for each source at each frequency setting, and visually inspected for emission. Also, spectra were extracted at the position of the radio nucleus, and inspected for emission. In all spectra the theoretical noise level was achieved. One potential problem with high frequency observations is phase coherence. To check the phase coherence, a continuum image of each source was synthesized. In both cases the continuum flux density observed was close to the expected value (determined by extrapolating a power law spectrum from lower frequencies to 22 GHz), and the spatial distribution agreed with that expected for each source.

The radio galaxy 1243+036 was also observed at OVRO during December 1994 and January 1995 at 100.5 GHz in redshifted CO(4–3). Four tracks were obtained in various configurations of the six telescopes, with interferometer baselines from 35 to 242 metres. During every track 1243+036 was observed for a total time of about 8 hours. Phases were calibrated using 3C 273 which was observed every 30 minutes. Once every hour, measurements of 3C 273 were also done to correct the pointing. 3C 273 was also used as a passband calibrator. The flux density scale was calibrated with measurements of 3C 84, 3C 454.3, 0528+134, Neptune and Uranus. The backend was configured with four adjacent and slightly overlapping bands, each covering 128 MHz in 32 channels. The CO(4–3) line from 1243+036 was searched for in lower side band (LSB) at 100.5 GHz. System temperatures were typically 200 K (SSB). After standard editing and calibration, AIPS was used to produce the final data cube at a spectral resolution of 32 MHz (96 km s^{-1}). The OVRO beam size at 100 GHz was about 2″

The interferometric observations with the achieved noise levels are summarized in Table 3.

3. Results

3.1. Limits on CO emission from single dish observations

A number of features were observed that significantly exceeded the noise level in the rest of the spectrum and remained when the receivers were tuned to different offset velocities. We first concluded that such features, at a level of a few mK, were real CO emission features. However, none of these features could be reproduced in different observing sessions. When re-observed, there was no evidence for any emission down to lower noise levels or new features appeared at a different frequency. Examples of this situation are shown in Figs. 1 and 2. Thus the observed features in the spectra were not due to line emission but were instrumental artefacts. The ability to detect faint broad emission lines depends strongly on these instrumental features in a spectrum and not only on the formal noise level. A discussion of these effects in the JCMT spectra has been given by Röttgering et al. (1995b).

We determined the final r.m.s. noise level of the spectra at a velocity resolution of 100 km s^{-1} over the entire observed velocity range (thus also including any possible spurious features) and these noise levels are listed in Table 2. Because of the occurrence of spurious features, some spectra with relatively short integration times but no spurious features have lower effective noise levels than other spectra with longer total integration times but with spurious features.

From the noise levels we estimate upper limits for the line flux from the objects. If we assume that a CO emission line has a Gaussian shape with a specific FWHM, we estimate a 2σ upper limit to the CO flux as $1.06 \times \mathrm{FWHM} \times 2 \times \sigma_{100}$ where σ_{100} is the r.m.s noise in the coadded spectrum at a velocity resolution of 100 km s^{-1}. We assume a FWHM of 300 km s^{-1} as for the observed lines in IRAS F10214+4724 and the Cloverleaf quasar (Solomon et al. 1992a, Barvainis et al. 1994). From the line flux limits we derive a 2σ upper limit on the CO luminosity based on the lowest CO transition observed under good

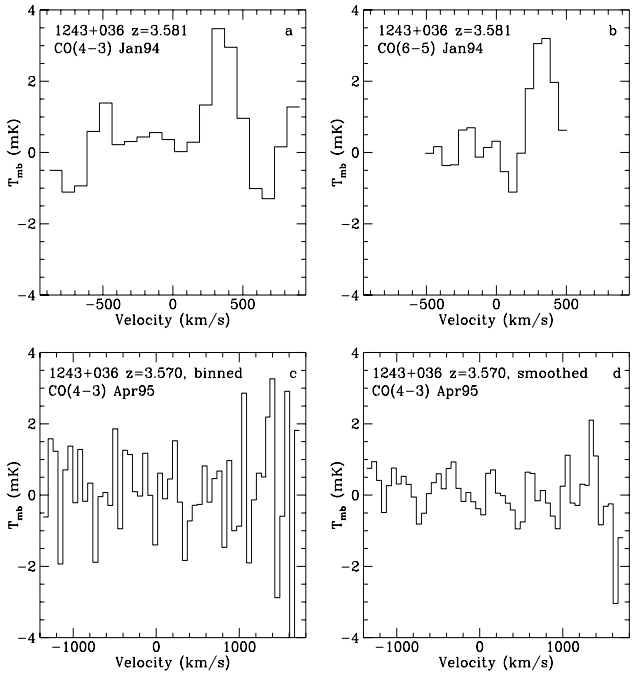

Fig. 1a–d. CO $J = 4 \rightarrow 3$ (**a**) and $J = 6 \rightarrow 5$ (**b**) spectra of the radio galaxy 1243+036 observed with the IRAM 30 m telescope in January 1994. The spectra are centred at the redshift of Lyα from a low resolution optical spectrum, were smoothed with a 100 km s^{-1} FWHM Gaussian and block-averaged into bins of $\sim$ 85 km s^{-1}. Both in the 3 mm (a) and the 2 mm (b) spectrum a feature was observed at an offset velocity of $\sim$ 320 km s^{-1} from the optical redshift. In spectra with different LO settings these features were present at a constant sky frequency as expected for an astronomical emission line. The same object was observed in April 1995 with the IRAM 30m telescope in CO $J = 4 \rightarrow 3$ ((**c**) and (**d**)). The centre is now at a corrected redshift from a high resolution optical spectrum. We have extended the baseline by adding many overlapping spectra with LO settings up to 600 km s^{-1} from the redshifted sky frequency. In spectrum (**c**) the data was block-averaged into bins of 65 km^{-1}. In spectrum (**d**), the data were first smoothed with a 100 km s^{-1} FWHM Gaussian and then rebinned. The feature seen in January 1994 should have appeared at +1050 km s^{-1}. No evidence for any emission feature is seen in (**c**) and (**d**), leading to the conclusion that the tentative result from the earlier observations (**a**) and (**b**) was spurious.

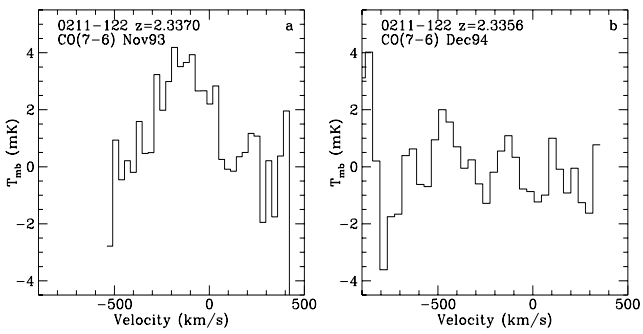

Fig. 2. a Spectrum of CO(7–6) of the radio galaxy 0211−122 observed with the JCMT in November 1993. This spectrum includes only the data with atmospheric transparency $\tau < 0.1$, i.e. from 4 of the 6 shifts (where one shift is 8 hours). There appears to be a strong emission feature centred at -150 km s^{-1} from the optical redshift. **b** Spectrum of CO(7–6) of 0211−122 taken with the JCMT in December 1994, centred at the tentative emission feature from spectrum (**a**). We have extended the baseline by combining spectra with 5 different LO settings to better distinguish any emission features. The tentative emission feature is of (**a**) absent in (**b**). Both spectra have been smoothed with a 100 km s^{-1} FWHM Gaussian and block-averaged into bins of $\sim$ 60 km s^{-1}.

atmospheric conditions, using the following formula, which is independent of beam size (see Solomon et al. 1992a):

$$L'_{\rm CO} = 3.25 \times 10^7 \, S_{\rm CO}\Delta v \, \nu_{\rm obs}^{-2} \, D_{\rm L}^2 \, (1+z)^{-3}, \qquad (1)$$

where $S_{\rm CO}\Delta v$ is the integrated line flux limit in Jy km s^{-1}, $\nu_{\rm obs}$ is the observing frequency in GHz, $D_{\rm L}$ the luminosity distance to the object in Mpc and the line luminosity L' is expressed in K km s^{-1} pc^2. The limits derived for the CO transitions used are listed in Table 4.

3.2. Limits on CO and dust emission from interferometric observations

No emission was seen in any spectral channel for either of the two objects observed with the VLA and OVRO. We derived 2σ upper limits for the CO luminosity for the interferometric observations in the same way as for the single dish observations. The limits are listed in Table 4.

The VLA continuum maps derived from the observations of 1243+036 (25 GHz) and 1435+635 (22 GHz) do show continuum emission. In 1243+036 there is a continuum peak of 3.5 mJy beam^{-1} at the location of the brightest hot spot seen in 8 GHz radio imaging observations (van Ojik et al.1996a). The continuum emission of 1435+635 has a peak of 2.5 mJy beam^{-1} and shows structure similar to the 8 GHz radio image. The continuum flux densities are consistent with non-thermal emission from the radio sources extrapolated using the spectral index determined between 8 GHz to 22 GHz. Thermal dust emission, as was recently detected from 1435+635 (Ivison 1995), would at a rest frequency of 115 GHz only be expected at the μJy level (estimated from the spectrum of Ivison 1995). The radio continuum is at the level of $\sim$ 3 mJy at this frequency. Thus any emission from dust is negligible compared to the synchrotron radio emission.

No continuum emission was observed in the 100 GHz continuum map derived from the OVRO observations of 1243+036 to a 2σ upper limit of 0.4 mJy beam^{-1}.

Table 4. 2σ upper limits on CO luminosity and molecular gas mass

Source	Line	z	line luminosity [K km s^{-1} pc^2]	$M(H_2)$ [10^{11} M$_\odot$]
Limits from the single dish observations				
0211−122	CO(3–2)	2.336	$< 2.4 \times 10^{10}$	< 1.0
0214+183	CO(6–5)	2.131	$< 4.1 \times 10^{10}$	< 1.6
0355−037	CO(6–5)	2.153	$< 4.1 \times 10^{10}$	< 1.7
0448+091	CO(6–5)	2.040	$< 2.1 \times 10^{10}$	< 0.8
4C 41.17	CO(4–3)	3.800	$< 1.3 \times 10^{10}$	< 0.5
0748+134	CO(3–2)	2.410	$< 1.0 \times 10^{10}$	< 0.4
0828+193	CO(3–2)	2.572	$< 3.2 \times 10^{10}$	< 1.3
B2 0902+34	CO(4–3)	3.395	$< 1.3 \times 10^{10}$	< 0.5
0943−242	CO(8–7)	2.918	$< 2.6 \times 10^{10}$	< 1.0
1243+036	CO(4–3)	3.570	$< 1.3 \times 10^{10}$	< 0.5
1435+635	CO(4–3)	4.257	$< 1.1 \times 10^{10}$	< 0.5
1707+105	CO(3–2)	2.345	$< 1.8 \times 10^{10}$	< 0.7
2202+128	CO(8–7)	2.704	$< 2.3 \times 10^{10}$	< 0.9
2251−089	CO(6–5)	2.000	$< 3.5 \times 10^{10}$	< 1.4
Limits from the interferometric observations				
1243+036	CO(4–3)	3.570	$< 1.0 \times 10^{10}$	< 0.4
1243+036	CO(1–0)	3.570	$< 6.5 \times 10^{10}$	< 3.3
1435+635	CO(1–0)	4.257	$< 2.8 \times 10^{10}$	< 1.3

4. Discussion

4.1. Limits on the molecular gas masses

For Galactic giant molecular clouds the relation between CO luminosity and H_2 mass has been determined as

$$\alpha = M(H_2)/L'_{CO} = 2.2 n_{H_2}^{1/2}/T_b = 4.78 \quad (2)$$

(Solomon et al. 1992a), where T_b is the intrinsic line brightness temperature (which is constant for thermalized, opaque lines from different rotational levels), n_{H_2} is the H_2 density in cm^{-3}, $M(H_2)$ is the H_2 mass in M$_\odot$ and L'_{CO} has been given in Eq. (1). The conversion factor α depends on the excitation conditions of the molecular gas and may be either higher or lower in extremely luminous and active galaxies such as IRAS F10214+4724 and HZRGs than in the Milky Way. More fundamentally, in order to be able to trace H_2 with CO lines, the molecular gas must be enriched, and, while subsolar CO abundances are allowed, the CO column densities must be sufficient to produce optically thick ^{12}CO lines. Solomon et al. (1992a) show that for IRAS F10214+4724 the conversion factor α for the higher CO transitions is similar to the Galactic value of 4.78 for CO $J = 1 \rightarrow 0$. Using their value $\alpha \approx 4$ for the lowest CO transitions observed under good conditions, we derive upper limits for the (enriched) H_2 masses for our 14 HZRGs of slightly less than 10^{11} M$_\odot$. For consistency, we have used the same value for the CO-H_2 conversion for the limits from the interferometric observations of CO(1–0), because it differs only little from the Galactic value of 4.78. The upper limits for the CO luminosity and the corresponding H_2 mass are listed in Table 4.

The limits on the H_2 masses that we find are marginally smaller than the molecular gas mass that was initially estimated for IRAS F10214+4724 (10^{11} M$_\odot$ before it was realized that it is lensed. In low redshift radio galaxies, Mazzarella et al. (1993) found molecular gas masses of order 10^{10} M$_\odot$. Thus, we find that radio galaxies at high redshifts are not much more gas-rich than those at low redshifts. As a prototypical gas-rich starburst galaxy and ultra-luminous IRAS galaxy (ULIRG) at low redshift, Arp 220 has a large molecular mass, $M(H_2) \sim 2 \times 10^{10}$ M$_\odot$ (Solomon et al. 1990 and references therein). Although it is possible that our HZRGs contain amounts of molecular gas similar to the ULIRGs, they cannot contain much more.

4.2. Implications of these and other millimetre observations at high redshift

The two high z objects with confirmed detections of emission from molecular gas, IRAS F10214+4724 and the cloverleaf quasar, are both gravitationally lensed. This could explain why the present and other searches for molecular gas in high redshift galaxies and quasars have been unsuccessful so far and might be taken as a discouragement for further searches. However, for the two objects detected the lensing amplification is unlikely to be much more than a factor of 10–20 (Barvainis et al. 1994), which, although rendering the true CO flux density too low for current instrumentation, may be observable in the future. The amplification of the flux densities of IRAS F10214+4724 and the Cloverleaf quasar imply that the underlying systems are not necessarily of extraordinary properties. Although still quite luminous and with $\sim 10^{10}$ M$_\odot$ of molecular gas quite gas-rich galaxies, they may well be "normal" active galaxies in the early universe, so that that many active galaxies, quasars and radio galaxies at high z may contain similar amounts of molecular gas.

The detection of submillimetre continuum emission from a number of high redshift radio galaxies and quasars in several searches (McMahon et al. 1994, Dunlop et al. 1994, Isaak et al. 1994, Ivison 1995) has been used to estimate gas masses using simple assumptions on the dust temperature and gas/dust ratio. The estimates of molecular gas masses of $0.5 - 1 \times 10^{11}$ M$_\odot$ from these continuum observations are not in contradiction with the non-detections of molecular gas in these objects and our sample of HZRGs. Far-infrared luminosities of $10^{13} - 10^{14}$ L$_\odot$, as implied by the submillimetre dust detections, imply star formation rates of $10^3 - 10^4$ M$_\odot$ yr^{-1} if the FIR luminosity is powered by star formation. By extrapolating from the somewhat lower luminosity ($L_{FIR} > 10^{12}$ L$_\odot$) ultra-luminous IRAS galaxies (Sanders et al. 1986), a value L_{FIR}/M_{H_2} of $100 - 1000$ L$_\odot$/M$_\odot$ is expected at these luminosities. The implied molecular masses are of the order of 10^{11} M$_\odot$, only slightly more than the present upper limits.

One of the explanations proposed for the strong alignment of the optical, near-infrared and radio axes of HZRGs (Chambers et al. 1987, McCarthy et al. 1987) is that vigorous starbursts are associated with the propagation of the radio jet (Rees 1989, Begelman & Cioffi 1989). In some of these radio

jet-induced star formation scenarios, star formation rates of the order of $10^4\,M_\odot\,yr^{-1}$ over a period of $\sim 10^8$ yrs are invoked to explain the alignment effect (Chambers & Charlot 1990, Chambers et al. 1990). Such star formation rates would imply that a mass of order $10^{12}\,M_\odot$ in (molecular) gas is converted into stars. The fact that we do not observe such quantities of (enriched) molecular gas in any high redshift radio galaxy is relevant to this scenario and can have two explanations:

1. The HZRGs that we observe have already consumed most of their molecular gas and formed the bulk of their stellar population. Jet-induced star formation may have played a role, but we are observing the object in a later phase where the radio source has already expanded into a powerful Faranoff-Riley II (FR-II) type source with an aligned stellar component in the galaxy hosting the radio source. Mazzarella et al. (1993) found molecular gas in several low redshift radio galaxies detected with IRAS, but not in the most powerful FR-II radio galaxies. They suggested that the powerful FR-II galaxies might be in a later phase where most of the molecular gas has been converted into stars.
2. The alignment effect may not be due to jet-induced star formation, but to another mechanism (cf., McCarthy 1993 for a review) such as scattering of continuum radiation emitted along the radio axis from a hidden AGN (Tadhunter et al. 1992, Cimatti et al. 1993, Di Serego Alighieri et al. 1994), anisotropic density distributions in the surrounding gas (Eales 1992) and inverse Compton scattering (Daly 1992). The passage of the radio jet still enhances star formation, but star formation would be not much more than in local starburst galaxies, up to $\sim 100\,M_\odot\,yr^{-1}$.

The possibility of a large amount of very cold molecular mass (temperature of a few K, as in the inner disk of M31, Allen & Lequeux 1993) is ruled out, because the gas cannot be colder than the cosmic microwave background which is 10 K at $z \sim 2.5$, so that CO lines up to $J = 3\rightarrow2$ would always be relatively strong (Solomon et al. 1992b). Although such cold gas may show no emission from the higher CO transitions, the lack of CO(1–0) and CO(3–2) emission observed in our data indicates that even if the CO is cold, there must be less than $\sim 10^{11}\,M_\odot$ in molecular gas.

It is unlikely that metallicity effects play a major role. The CO-H_2 conversion factor α scales with CO abundance $X(\mathrm{CO})$ approximately as $\alpha \propto [X(\mathrm{CO})]^{-1/4}$ (Radford et al. 1991; Solomon et al. 1992a) as long as the CO lines are optically thick. Abundance effects thus only begin to play a role when the CO lines become optically thin, which requires an abundance of several orders of magnitude below solar. While this situation cannot be ruled out, the presence of large masses of dust as revealed by thermal submm emission in several of our targets, and the high metallicities indicated by the optical spectrum of 0211−122 (Van Ojik et al. 1994) indicate otherwise. Simultaneously, the dust will shield the molecules from dissociation by the UV continuum, as is also the case in IRAS F10214+4724 and the Cloverleaf quasar (cf., Sect. 1).

5. Summary and conclusions

We have searched for CO emission in a sample of 14 high redshift radio galaxies between $z = 2$ and 4.3. In none of these galaxies have we found consistent evidence for CO emission.

For a CO-H_2 conversion factor similar to the Galactic value, we find 2σ upper limits to the molecular mass of less than $10^{11}\,M_\odot$. The upper limits to the molecular gas mass in HZRGs suggests that they are not forming stars at rates of $\sim 10^4\,M_\odot\,yr^{-1}$ which was previously suggested in some jet induced star formation scenarios to explain the optical-radio alignment effect. This may mean that (i) all powerful HZRGs have already converted their gas into stars, possibly through jet induced star formation, or (ii) jet induced star formation does not play an important role in the alignment effect but HZRGs may still be star forming at the rate of local starburst galaxies.

Acknowledgements. These observations would not have been possible without the good support of the staff at the IRAM 30 m telescope and the James Clerk Maxwell Telescope. We thank Nick Scoville and Min Yun for carrying out the OVRO observations and for useful discussions. The James Clerk Maxwell Telescope is operated by The Observatories on behalf of the Particle Physics and Astronomy Research Council of the United Kingdom, the Netherlands Organization for Scientific Research, and the National Research Council of Canada. OVRO is operated under funding from the U.S. National Science Foundation, grant 93-14079. The VLA is a facility of the U.S. National Radio Astronomy Observatory, which is operated by Associated Universities, Inc., under cooperative agreement with the U.S. National Science Foundation. We acknowledge support from an EC twinning project and a programme subsidy granted by the Netherlands Organization for Scientific Research (NWO). The research of Van der Werf has been made possible by the Royal Netherlands Academy of Arts and Sciences.

References

Allen, R.J., Lequeux, J., 1993, ApJ 410, L15
Antonucci, R., 1993, ARA&A 31, 473
Barvainis, R., Tacconi, L., Antonucci, T., et al., 1994, Nat 371, 586
Begelman, M.C., Cioffi, D.F., 1989, ApJ 345, L21
Braine J., Downes D., Guilloteau S., 1996, ApJ, 309, L43
Broadhurst, T., Lehár, J., 1995, ApJ, 450, L41
Brown, R.L., Vanden Bout, P.A., 1991, AJ 102, 1956
Brown, R.L., Vanden Bout, P.A., 1993, ApJ 412, L21
Chambers, K.C., Charlot, S., 1990, ApJ 348, L1
Chambers, K.C., Miley, G.K., Van Breugel, W., 1987, Nat 329, 604
Chambers, K.C., Miley, G.K., Van Breugel, W.J.M., 1990, ApJ 363, 21
Chini, R., Krügel, E., 1994, A&A 288, L33
Cimatti, A., Di Serego Alighieri, S., Fosbury, R.A.E., et al. 1993, MNRAS 264, 421
Daly, R., 1992, ApJ 399, 426
Di Serego Alighieri, S., Cimatti, A., Fosbury, R.A.E., 1994, ApJ 431, 123
Dunlop, J.S., Hughes, D.H., Rawlings, S., Eales, S.A., Ward, M.J., 1994, Nat 370, 347
Eales, S.A., 1992, ApJ 397, 49
Eales, S.A., Rawlings, S., 1993, ApJ 411, 67
Elston, R., McCarthy, P.J., Eisenhardt, P., et al., 1994, ApJ 107, 910
Frayer, D.T., Brown, R.L., & Vanden Bout, P.A., 1994, ApJ 433, L5

Graham, J.R., Liu M.C., 1995, ApJ, 449, L29
Isaak, K.G., McMahon R.G., Hills, R., Withington, S., 1994, MNRAS 263, L28
Ivison, R.J., 1995, MNRAS, 275, L33
Lacy, M., Miley, G.K., Rawlings, S., et al., 1994, MNRAS 271, 504
Lilly, S., 1988, ApJ 333, 161
McMahon, R.G., Omont, A., Bergeron, J., et al., 1994, MNRAS 267, L9
Mazzarella, J.M., Graham, J.R., Sanders, D.B., Djorgovski, S., 1993, ApJ 409, 370
McCarthy, P.J., Van Breugel, W., Spinrad, H., Djorgovski, S., 1987, ApJ 321, L29
McCarthy, P.J., 1993, ARA&A 31, 639
Radford, S.J.E., Solomon, P.M., Downes, D., 1991, ApJ 369, L15
Rees, M.J., 1989, MNRAS 239, 1P
Röttgering H., Hunstead R., Miley G. K., van Ojik R., Wieringa M. H., 1995a, MNRAS, 277, 389
Röttgering H., Jenness T., Sleath J., Miley G., van Ojik R., van der Werf P., 1995b, JCMT Newsletter, March, 32
Röttgering H., van Ojik R., Miley G., Chambers K., van Breugel W., de Koff S., 1997, A & A: in press
Rowan-Robinson, M., Broadhurst, T., Lawrence, A., et al., 1991, Nat 351, 719
Sanders, D.B., Scoville, N.Z., Young J.S., et al., 1986, ApJ 305, L45
Solomon, P.M., Radford, S.J.E., Downes, D., 1990, ApJ 348, L53
Solomon, P.M., Downes, D., Radford, S.J.E., 1992a, ApJ 398, L29
Solomon, P.M., Radford, S.J.E., Downes, D., 1992b, Nat 356, 318
Tadhunter, C.N., Scarrott, S., Draper, P., Rolph, C., 1992, MNRAS 256, 53p
Van der Werf, P.P., Israel, F.P., 1996, In: Shaver, P. (ed.) Science with Large Millimetre Arrays. Springer, in press
van Ojik R., Röttgering H., Miley G., Bremer M., Macchetto F., Chambers K., 1994, A&A, 289, 54
van Ojik R., Röttgering H., Carilli C., Miley G., Bremer M., 1996a, A&A, 313, 25
van Ojik R., Röttgering H. J. A., Miley G. K., Hunstead R., 1997, A&A: in press
Wiklind, T., Combes, F., 1994, A&A 288, L41

This article was processed by the author using Springer-Verlag LaTeX A&A style file *L-AA* version 3.